International Journal of Engineering & Technology, 7 (4.3) (2018) 64-70

International Journal of Engineering & Technology

Website: www.sciencepubco.com/index.php/IJET

Research paper

Analysis of Various Approaches to Modeling of Dynamics of Lifting-Transport Vehicles

Otto Grigorov[1]*, Evgenij Druzhynin[2], Galina Anishchenko[2], Marjana Strizhak[1], Vsevolod Strizhak[1]

[1] *Institute of Mechanical Engineering and Transport*
[2] *Engineering Physics Institute*
**Corresponding author E-mail: galaanishchenko@gmail.com, druzhinin_e_i@ukr.net, stryzhak.vsevolod@gmail.com*

Abstract

The results of analytical and numerical modeling of dynamic characteristics of linear and non-linear mathematical models of the "trolley-load" system of bridge and container cranes are presented. KiDyM software complex is used for numerical modeling, which, based on the use of the apparatus of structural matrices and the built-in computer algebra system, allows the construction of ordinary differential equations of motion of the class of systems under consideration at the analytical level. Recommendations on the possible use of the considered mathematical models of the "trolley-load" system in various regular and forced operation modes of bridge and container cranes are given on the basis of the analysis. The ratio of the results of calculations for various design models of regular and forced operation of the bridge crane has been established. The magnitude of the distribution of the maximum values of the dynamic characteristics of motion of the container crane has been designed by calculating the forced operation mode using various mathematical models.

Keywords: *bridge crane; hydrostatic drive; movement mechanism; optimal control; power drive.*

1. Introduction

Increasing the efficiency of the use of lifting machines requires the improvement of the design as a whole and its individual units, as well as improving the control of the truck crane movement.
Introduction of the optimal automatic control is a rather challenging task. This can be explained by the relatively small number of operating systems on real cranes compared with the numerous scientific developments on this problem that have been accumulated in the world for decades since its appearance. [1] Today, the problem of suppression of load oscillation is solved largely by experienced crane operators, the space suspension of the load, or through the introduction of special crane designs that prevent a flexible suspension, for example, a port bridge crane with a retractable high jibs and balancing cranes. [2] In some cases optimal control is replaced by quasi-optimal, which allows for certain predetermined errors, but is much easier to implement, renouncing feedback. The search for ways of simplification has also involved mathematical models - the basis for constructing the laws of optimal movement of the trolley-load system [3]. Today, there are a number of models that describe the movement of this system [4]. Some of them were obtained more than 50 years ago and are still used today. However, the simplification of the mathematical model may not always be acceptable, for example, for container cranes, where optimality of control is one of the main requirements, and the deviation of load positioning should not exceed 10-20 mm at high speeds of movement of the trolley (up to 240 m/min.), a significant length of the suspension (up to 40 m) and a large weight of the load with a spreader. Simpler models can be used with lower accuracy requirements [5]. Practice has proved that the calculated dynamic characteristics of the trolley-load system can differ by more than 2.5 times, depending on the chosen approach.

2. Comparison of Mathematical Models of the "Trolley-Load" System

The current scientific and practical task is comparing different mathematical models of the "trolley-load" system in order to identify among them those that most adequately describe the dynamics of lifting and handling machinery (LHM). The purpose can be achieved by numerical integration of various existing models under the same conditions and operating modes.

2.1. Model 1.

Kinetic energy of the system:

$$T = T_1 + T_2,$$

where $T_1 = \frac{m_1 \dot{x}_1^2}{2}$; $T_2 = \frac{m_2 v_a^2}{2}$;

$$v_a^2 = v_e^2 + v_r^2 + 2 v_e v_r \cos\left(180^2 - \varphi\right) =$$
$$= \dot{x}^2 + l^2\dot{\varphi}^2 - 2\dot{x}l\dot{\varphi}\cos\varphi,$$

then

$$T = \frac{m_1 \dot{x}^2}{2} + \frac{m_2\left(\dot{x}^2 + l^2\dot{\varphi}^2 - 2\dot{x}l\dot{\varphi}\cos\varphi\right)}{2}.$$

Energy dissipation system (Rayleigh function):

$$\Phi = \beta\frac{\dot{\varphi}^2}{2};$$

Potential energy of the system:
$\Pi = -m_2 g l \cos\varphi;$

Lagrange equations:

$$\begin{cases} \dfrac{d}{dt}\left(\dfrac{\partial T}{\partial \dot{x}}\right) - \dfrac{\partial T}{\partial x} = Q_x; \\ \dfrac{d}{dt}\left(\dfrac{\partial T}{\partial \dot{\varphi}}\right) - \dfrac{\partial T}{\partial \varphi} = Q_\varphi - \dfrac{\partial \Phi}{\partial \dot{\varphi}}, \end{cases} \quad (1)$$

here x, φ – generalized coordinates; $\dot{x}$, $\dot{\varphi}$ – generalized velocities;

Q_x, Q_ϕ, $\dfrac{\partial \Phi}{\partial \dot{\varphi}}$ – generalized forces.

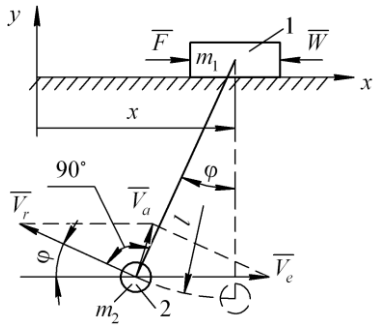

Fig. 1: Scheme for model 1:1 - trolley, 2 - load, m_1 - trolley weight, m_2 - load weight, φ – swing angle of load, F - driving force, W - resistance to movement, V_a – absolute velocity, V_r - relative velocity, V_e - transport velocity.

We calculate partial derivatives of kinetic energy by generalized velocities and coordinates:

$$\frac{\partial T}{\partial \dot{x}} = m_1 \dot{x} + m_2\left(\dot{x} - l\dot{\varphi}\cos\varphi\right);$$

$$\frac{\partial T}{\partial \dot{\varphi}} = m_2\left(l^2\dot{\varphi} - \dot{x}l\cos\varphi\right) = m_2 l\left(l\dot{\varphi} - \dot{x}\cos\varphi\right);$$

$$\frac{\partial T}{\partial x} = 0; \quad \frac{\partial T}{\partial \varphi} = m_2 \dot{x} l \dot{\varphi}\sin\varphi.$$

Determination of the complete derivatives of the time from the partial derivatives:

$$\frac{d}{dt}\left(\frac{\partial T}{\partial \dot{x}}\right) = (m_1 + m_2)\ddot{x} - m_2 l\left(\cos\varphi\cdot\ddot{\varphi} - \sin\varphi\cdot\dot{\varphi}^2\right);$$

$$\frac{d}{dt}\left(\frac{\partial T}{\partial \dot{\varphi}}\right) = m_2 l\left[l\ddot{\varphi} - \left(\ddot{x}\cos\varphi - \dot{x}\dot{\varphi}\cdot\sin\varphi\right)\right] =$$
$$= m_2 l\left[l\ddot{\varphi} - \cos\varphi\cdot\ddot{x} + \sin\varphi\cdot\dot{x}\cdot\dot{\varphi}\right].$$

We find generalized forces:

$$Q_x = F - W\cdot sign(\dot{x}); \quad Q_\varphi = -\frac{\partial \Pi}{\partial \varphi} = -m_2 g l\sin\varphi; \quad \frac{\partial \Phi}{\partial \dot{\varphi}} = \beta\dot{\varphi}.$$

Obtained expressions will be substituted in (1):

$$\begin{cases} (m_1 + m_2)\ddot{x} - m_2 l\cos\varphi\cdot\ddot{\varphi} + m_2 l\cdot\sin\varphi\cdot\dot{\varphi}^2 = \\ = \text{F-W}\cdot\text{sign}(\dot{x}); \\ m_2 l\left[l\ddot{\varphi} - \cos\varphi\cdot\ddot{x} + \sin\varphi\cdot\dot{\varphi}\dot{x}\right] - m_2 l\cdot\sin\varphi\cdot\dot{x}\dot{\varphi} = \\ = -m_2 l\,g\sin\varphi - \beta\dot{\varphi}. \end{cases} \quad (2)$$

After elementary transformations we have:

$$\begin{cases} (m_1 + m_2)\ddot{x} - m_2 l\cos\varphi\cdot\ddot{\varphi} + m_2 l\sin\varphi\cdot\dot{\varphi}^2 = \text{F-W}\cdot\text{sign}(\dot{x}); \\ l\ddot{\varphi} - \cos\varphi\cdot\ddot{x} + \beta\dot{\varphi} + g\sin\varphi = 0. \end{cases} \quad (3)$$

2.2. Model 2.

For small oscillation amplitudes:
$\sin\varphi \approx \varphi; \quad \cos\varphi \approx 1; \quad \sin\varphi\cdot\dot{\varphi}^2 \approx \varphi\cdot\dot{\varphi}^2 = 0;$

$$\begin{cases} (m_1 + m_2)\ddot{x} - m_2 l\ddot{\varphi} = \text{F-W}\cdot\text{sign}(\dot{x}); \\ l\ddot{\varphi} - \ddot{x} + \beta\dot{\varphi} + g\cdot\varphi = 0. \end{cases} \quad (4)$$

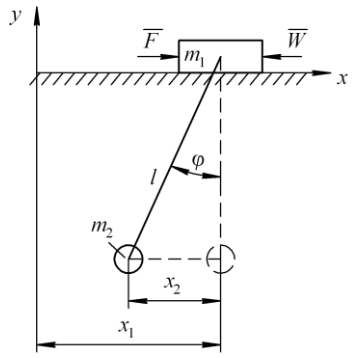

Fig. 2: Scheme for model 2.

If we put: $l\varphi = x_2, x = x_1$, then we obtain the equation in linear displacements:

$$\begin{cases} (m_1 + m_2)\ddot{x}_1 - m_2\ddot{x}_2 = \text{F-W}\cdot\text{sign}(\dot{x}_1); \\ \ddot{x}_2 - \ddot{x}_1 + \dfrac{\beta}{l}\dot{x}_2 + \dfrac{g}{l}x_2 = 0. \end{cases} \quad (5)$$

2.3. Model 3. Commonly Used Model (A)

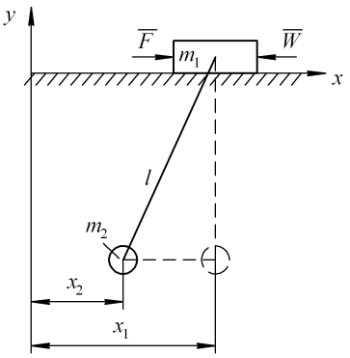

Fig. 3: Scheme for model 3.

x_2 – absolute movement of load;

$$\begin{cases} m_1\ddot{x}_1 + \dfrac{m_2 g}{l}\left(x_1 - x_2\right) = \text{F-W}\cdot\text{sign}(\dot{x}_1); \\ m_2\ddot{x}_2 - \dfrac{m_2 g}{l}\left(x_1 - x_2\right) = 0. \end{cases} \quad (6)$$

When integrating equations (6), a replacement of variables proposed by S.N. Kozhevnikov is desirable:

$$P_{12} = \frac{m_2 g}{l}\left(x_1 - x_2\right). \quad (7)$$

2.4. Model 4. Commonly Used Model (B)

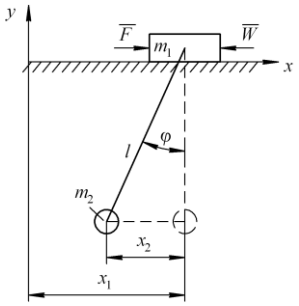

Fig. 4: Scheme for model 4.

x_2 – relative movement of cargo:

$$\begin{cases} m_1\ddot{x}_1 + \dfrac{m_2 g}{l} x_2 = \text{F-W}\cdot\text{sign}(\dot{x}_1); \\ m_2\left(\ddot{x}_2 - \ddot{x}_1\right) + \dfrac{m_2 g}{l} x_2 = 0. \end{cases} \quad (8)$$

In paragraphs 2.5, 2.6, we consider two more mathematical models of the crane-load system, in which the crane equation is replaced by an equation similar to the N.S. Haminin equation:

2.5. Model 5. Haminin-Lagrange

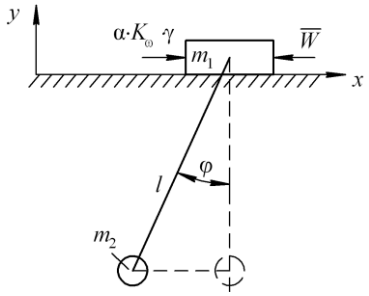

Fig. 5: Scheme for model 5.

$$\begin{cases} T_{mech}\ddot{x} + \dot{x} + T_{mech}\dfrac{m_2}{m_{12}}\cos\varphi\cdot l\cdot\ddot{\varphi} + T_{mech}\dfrac{m_2}{m_{12}}\sin\varphi\cdot l\dot{\varphi}^2 = \\ = \alpha\cdot K_\omega\gamma - \dfrac{W sign(\dot{x})}{F_{mech}}; \\ l\ddot{\varphi} - \cos\varphi\cdot\ddot{x} + \beta\dot{\varphi} + g\sin\varphi = 0. \end{cases} \quad (9)$$

2.6. Model 6. Haminin - commonly used model (A).

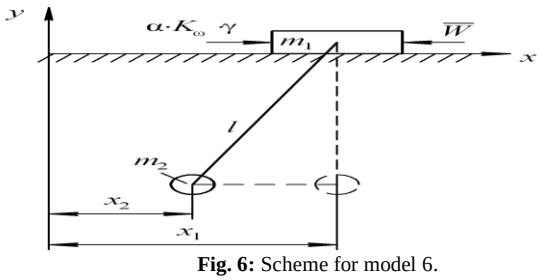

Fig. 6: Scheme for model 6.

$$\begin{cases} T_{mech}\ddot{x}_1 + \dot{x}_1 = \alpha\cdot K_\omega\gamma - \dfrac{W sign(\dot{x}_1)}{F_{mech}} - \dfrac{\text{m}_2 g}{l F_{mech}}\left(x_1 - x_2\right); \\ m_2\ddot{x}_2 - \dfrac{\text{m}_2 g}{l}\left(x_1 - x_2\right) = 0. \end{cases} \quad (10)$$

2.7 Stiffness of Mechanical Characteristic

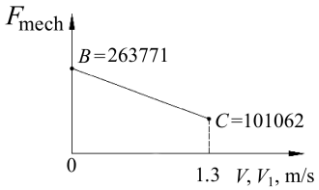

Fig. 7: Stiffness of mechanical characteristic.

$$F_{mech} = B - A\cdot V,$$

where $A = \dfrac{B-C}{1.3} = \dfrac{263771-101062}{1.3} = 125160.77.$

$$F_{mech} = 263771 - 125160.77\cdot V. \quad (11)$$

2.8 Frequency Spectrum of Models

Model 2: Linearized Lagrange equations

$$\begin{cases} \left(m_1 + m_2\right)\ddot{x} - m_2 l\ddot{\varphi} = 0; \\ l\ddot{\varphi} - \ddot{x} + g\cdot\varphi = 0, \end{cases} \quad (12)$$

Suppose that the solutions of the system of equations (12) have the form:

$$x = A_1\sin\left(\omega t + \alpha\right); \quad \varphi = A_2\sin\left(\omega t + \alpha\right); \quad (13)$$

then $$\ddot{x} = -A_1\omega^2\sin\left(\omega t + \alpha\right); \quad \ddot{\varphi} = -A_2\omega^2\sin\left(\omega t + \alpha\right). \quad (14)$$

Substituting (13) and (14) into (12), we obtain:

$$\begin{cases} -\left(m_1 + m_2\right)\omega^2 A_1 + m_2 l\omega^2 A_2 = 0; \\ \omega^2 A_1 + \left(g - l\omega^2\right)A_2 = 0. \end{cases} \quad (15)$$

The system (15) is homogeneous, therefore, a non-zero solution is possible only if the determinant is computed from the coefficients in the amplitudes, that is:

$$\begin{vmatrix} -\left(m_1 + m_2\right)\omega^2 & m_2 l\omega^2 \\ \omega^2 & g - l\omega^2 \end{vmatrix} = 0; \quad (16)$$

Having deployed a determinant, we obtain the frequency equation:

$$-\left(m_1 + m_2\right)\left(g - l\omega^2\right)\omega^2 - m_2 l\omega^4 = 0; \quad (17)$$

from which we will find two frequencies:

$$\omega_1 = 0; \quad \omega_2 = \sqrt{\frac{(m_1 + m_2)g}{m_1 l}}; \quad (18)$$

and with (15) we obtain the ratio of amplitudes of oscillations:

$$A_2 = \frac{m_1 + m_2}{m_2 l} A_1 \quad (19)$$

Model 3. Commonly Used Model - (A)

$$\begin{cases} m_1\ddot{x}_1 + \dfrac{m_2 g}{l}(x_1 - x_2) = 0, \\ m_2\ddot{x}_2 - \dfrac{m_2 g}{l}(x_1 - x_2) = 0. \end{cases} \quad (20)$$

Similarly to the previous model, we get:

$$x_1 = A_1\sin(\omega t + \alpha);\ x_2 = A_2\sin(\omega t + \alpha);$$
$$\ddot{x}_1 = -A_1\omega^2\sin(\omega t + \alpha);\ \ddot{x}_2 = -A_2\omega^2\sin(\omega t + \alpha);$$
$$\begin{cases} -m_1\omega^2 A_1 + m_2(g/l)(A_1 - A_2) = 0 \\ -m_2\omega^2 A_2 - m_2(g/l)(A_1 - A_2) = 0 \end{cases}$$
$$\begin{vmatrix} m_2 g/l - m_1\omega^2 & -m_2 g/l \\ -m_2 g/l & m_2(g/l - \omega^2) \end{vmatrix} = 0$$
$$m_1\omega^4 - (g/l)(m_1 + m_2)\omega^2 = 0\ ;$$
$$m_1\omega_2^2 - (g/l)(m_1 + m_2) = 0\ ;$$

$$\omega_1 = 0;\quad \omega_2 = \sqrt{\frac{(m_1 + m_2)g}{m_1 l}}; \quad (21)$$

$$A_2 = \frac{m_1}{m_2 l}A_1. \quad (22)$$

From the comparison of formulas (18), (21) and (19), (22) it is evident that the frequencies of models 2 and 3 coincide, and the ratio of amplitudes of oscillations are different.

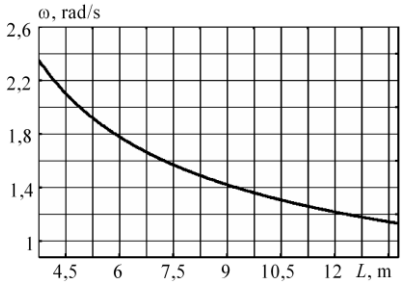

Fig. 8: Natural frequency of the "crane-load" system.

Figure 6 shows the dependence of the frequency of the free vibrations of the bridge crane on the length of the load suspension.

3. Numerical Modeling

To prepare for numerical simulation, we reduce equations (3) of model 1 to the Cauchy form. In the vector-matrix form, the system of equations (3) has the form:

$$A\ddot{\vec{x}} = \vec{B}. \quad (23)$$

If A has an inverse matrix A^{-1}, then, multiplying the left and right sides (23) on the left by A^{-1}, we obtain:

$$A^{-1}\cdot\ddot{\vec{x}} = A^{-1}\cdot\vec{B},$$

Or

$$E\cdot\ddot{\vec{x}} = A^{-1}\cdot\vec{B}. \quad (24)$$

Rewriting (3) in the form:

$$\begin{cases} m_{12}\ddot{x} - m_2 l\cos\varphi\cdot\ddot{\varphi} = \text{F-W}\cdot\text{sign}(\dot{\text{x}})\text{-}m_2 l\sin\varphi\cdot\dot{\varphi}^2; \\ -\cos\varphi\cdot\ddot{x} + l\ddot{\varphi} = -g\sin\varphi - \beta\dot{\varphi}. \end{cases} \quad (25)$$

where $m_{12} = m_1 + m_2$.

We denote:

$b_1 = F\text{-}W\cdot\text{sign}(\dot{\text{x}})\text{-}m_2 l\sin\varphi\cdot\dot{\varphi}^2;\ b_2 = -g\sin\varphi - \beta\dot{\varphi};$

The matrix A of the system (25) has the form:

$$A = \begin{pmatrix} m_{12} & -m_2 l\cos\varphi \\ -\cos\varphi & l \end{pmatrix}.$$

The inverse matrix elements:

$a_{ij}^* = \dfrac{(-1)^{i+j}\cdot A_{ji}}{\Delta}$, where A_{ji} – minors of the matrix A;

Δ –determinant of matrix A;

$\Delta = m_{12}l - m_2 l\cos^2\varphi = l\left(m_{12} - m_2\cos^2\varphi\right).$

Find the elements of the inverse matrix:

$a_{11}^* = 1/\left(m_{12} - m_2\cos^2\varphi\right);\ a_{12}^* = m_2\cos\varphi/\left(m_{12} - m_2\cos^2\varphi\right);$

$a_{21}^* = \cos\varphi/l\left(m_{12} - m_2\cos^2\varphi\right);\ a_{22}^* = m_{12}/l\left(m_{12} - m_2\cos^2\varphi\right).$

Then the system of equations (3) of model 1 in the form of Cauchy has the form:

$$\begin{cases} \dot{x}_1 = V_1; \\ \dot{V}_1 = a_1^*\cdot b_1 + a_{12}^*\cdot b_2; \\ \dot{\varphi} = \omega; \\ \dot{\omega} = a_{21}^*\cdot b_1 + a_{22}^*\cdot b_2. \end{cases} \quad (26)$$

Similarly, for model 2 (the system of equations (4)) the Cauchy form has the form (26), where

$a_{11}^* = 1/\left(m_{12} - m_2\right);\ m_{12} = m_1 + m_2;\ a_{12}^* = m_2/\left(m_{12} - m_2\right);$

$a_{21}^* = 1/l\left(m_{12} - m_2\right);\ a_{22}^* = m_{12}/l\left(m_{12} - m_2\right);\ b_1 = F - W\cdot sign(\dot{x});$

$b_2 = -(g\varphi + \beta\dot{\varphi}).$

Equations in the Cauchy form for model 3 with allowance for replacement of variables $P_{12} = \dfrac{m_2 g}{l}(x_1 - x_2)$, has the form:

$$\begin{cases} \dot{x}_1 = V_1; \\ \dot{V}_1 = b_1/m_1; \\ P_{12} = V_{12}; \\ \dot{V}_{12} = \dfrac{g}{l}\left(\dfrac{m_2}{m_1}\cdot b_1 - b_2\right), \end{cases} \quad (27)$$

where $b_1 = F - W\cdot sign(\dot{x}_1) - P_{12};\quad b_2 = P_{12}.$

For Model 4 we have:

$$\begin{cases} \dot{x}_1 = V_1; \\ \dot{V}_1 = b_1/m_1; \\ \dot{x}_2 = V_2; \\ \dot{V}_2 = b_1/m_1 + b_2/m_2, \end{cases} \quad (28)$$

where $b_1 = F - W\cdot sign(\dot{x}_1) - \dfrac{m_2 g}{l}x_2;\quad b_2 = -\dfrac{m_2 g}{l}x_2.$

For model 5, the form of Cauchy is represented by the system of equations (26), where

$$b_1 = \alpha K_\omega\cdot\gamma - \frac{W}{F_{mech}} - \dot{x} - T_{mech}\cdot\frac{\text{m}_2}{\text{m}_{12}}l\sin\varphi\cdot\dot{\varphi}^2;$$
$$b_2 = -g\sin\varphi - \beta\dot{\varphi};$$

$$a_{11}^{*}=1\Big/T_{mech}\left(1+\frac{\mathrm{m}_2}{\mathrm{m}_{12}}\cos^2\varphi\right);\quad a_{12}^{*}=-\frac{\left(m_2/m_{12}\right)\cdot\cos\varphi}{1+\left(\frac{m_2}{m_{12}}\cos^2\varphi\right)};$$

$$a_{21}^{*}=-\frac{\cos\varphi}{T_{mech}l\left(1+\frac{m_2}{m_{12}}\cos^2\varphi\right)};\quad a_{22}^{*}=-\frac{1}{l\left(1+\frac{m_2}{m_{12}}\cos^2\varphi\right)}.$$

For model 6, described by the system of equations (10), we have:

$$\begin{cases}\dot{x}_1=V_1;\\ \dot{V}_1=b_1/T_{mech};\\ P_{12}=V_{12};\\ \dot{V}_{12}=\dfrac{m_2g}{l}\left(b_1/T_{mech}+\mathrm{b}_2\right),\end{cases}\qquad(29)$$

where

$$P_{12}=\frac{m_2g}{l}\left(x_1-x_2\right);b_1=\alpha K_\omega\cdot\gamma-\dot{x}_1-(W+P_{12})/F_{mech};\mathrm{b}_2=P_{12}\ .$$

KiDyM software complex is used for numerical simulation, which allows the construction of equations of motion of systems described by a set of ordinary differential equations at the analytical level. Equations (26) - (29) were integrated using the Runge-Kutta-Merson method. Figures 9-20 show the graphs for changing the parameters characterizing the dynamics of the crane-load system described using the mathematical models considered.

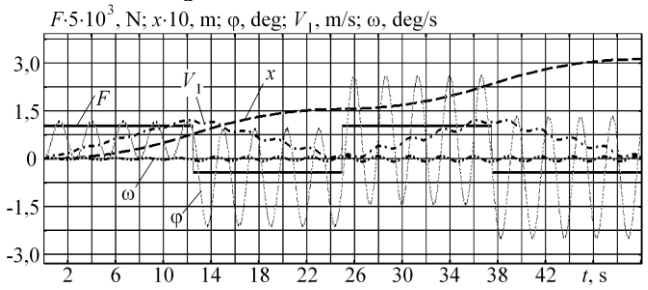

Fig. 9: Model 1. L=3 m, t_p=12.5 s.

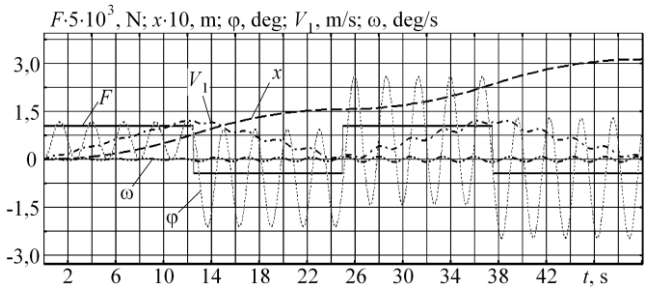

Fig. 10: Model 2. L=3 m, t_p=12.5 s.

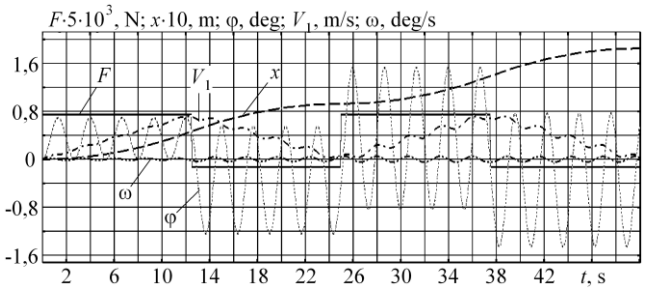

Fig. 11: Model 3. L=3 m, t_p=12.5 s.

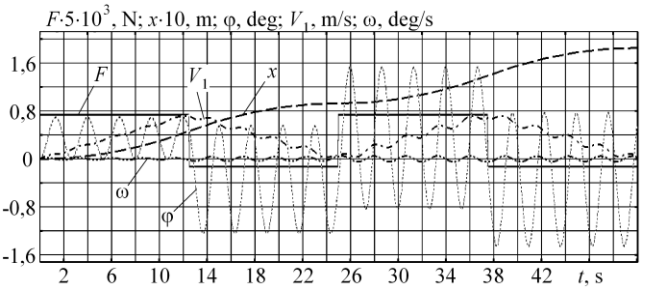

Fig. 12: Model 4. L=3 m, t_p=12.5 s.

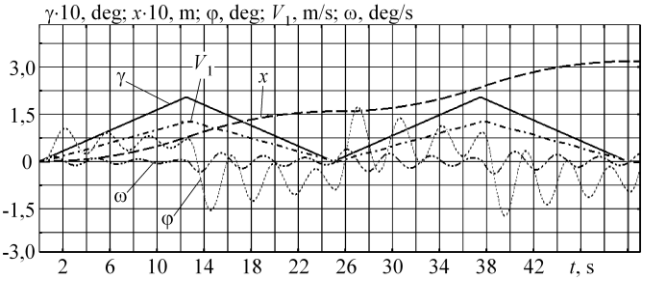

Fig. 13: Model 5. L=3 m, t_p=12.5 s.

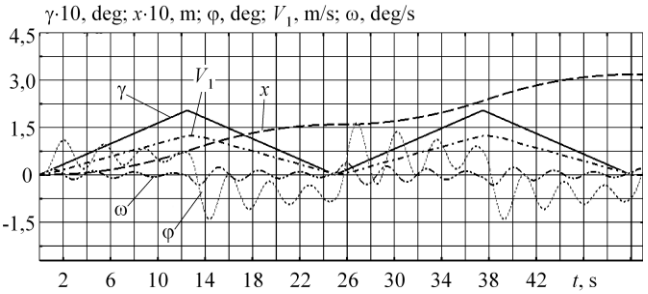

Fig. 14: Model 6. L=3 m, t_p=12.5 s.

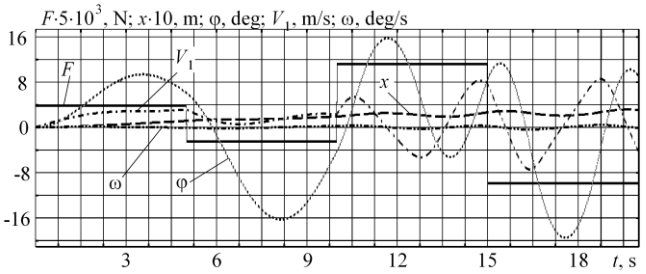

Fig. 15: Model 1. L=25 m, t_p=5 s.

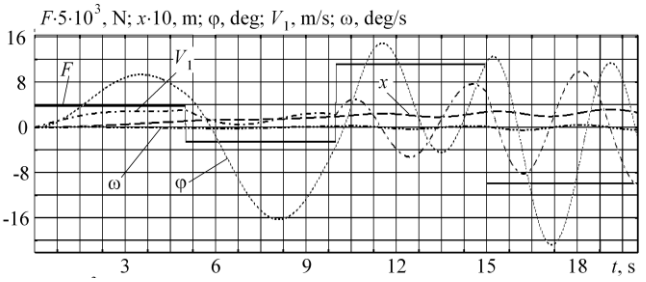

Fig. 16: Model 2. L=25 m, t_p=5 s.

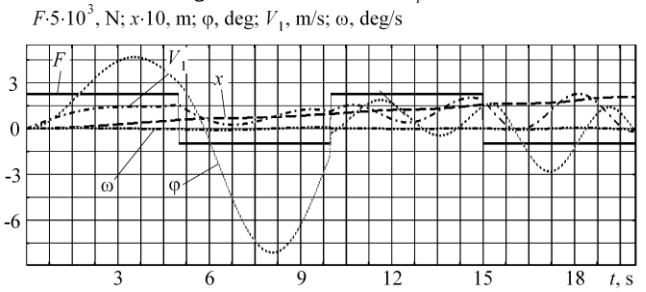

Fig. 17: Model 3. L=25 m, t_p=5 s.

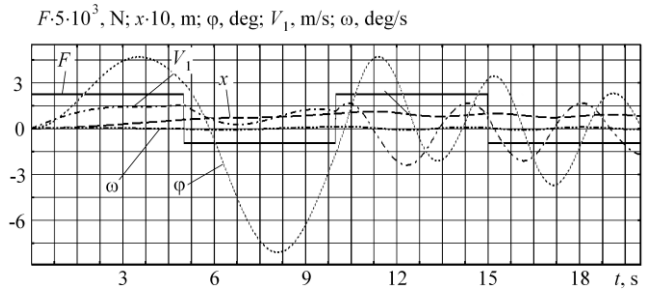

Fig. 18: Model 4. L=25 m, t_p=5 s.

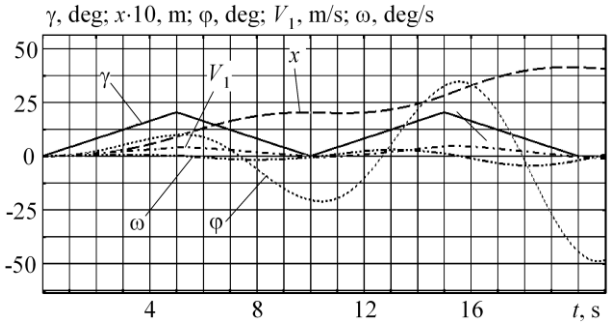

Fig. 19: Model 5. L=25 m, t_p=5 s.

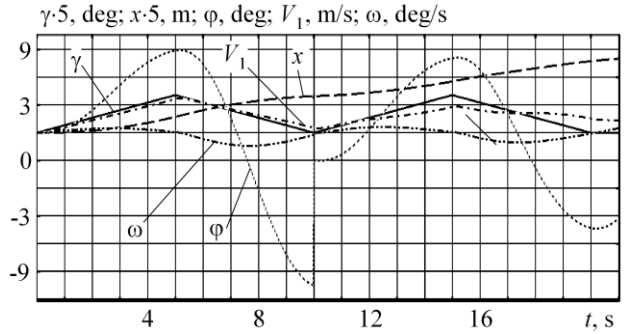

Fig. 20: Model 6. L=25 m, t_p=5 s.

The results of calculations of full-time and forced acceleration-deceleration modes of bridge and port cranes are given respectively in Tables 1 and 2.

Table 1: Results of calculations of full-time and forced acceleration-braking modes of a bridge crane

Model No.		Bridge crane			
		L=3, m t_p=6.28, s	L=3, m t_p=12.5, s	L=13, m t_p=6.28, s	L=13, m t_p=12.5, s
1	φ	3.248;-5.574	2.588;-1.418	2.325;-2.902	0.714;-1.881
	x	16.408	31.275	15.946	32.741
	ω	0.181;-0.181	0.082;-0.082	0.034;-0.034	0.026;-0.026
	v	1.296	1.220	1.337	1.308
2	φ	3.308;-5.62	2.582;-1.412	2.325;-2.898	0.714;-1.880
	x	16.409	31.270	15.931	32.739
	ω	0.183;-0.183	0.0821;-.082	0.034;-0.034	0.026;-0.026
	v	1.289	1.222	1.331	1.309
3	φ	1.795;-3.171	1.521;-0.836	1.374;-1.717	0.422;-1.112
	x	9.884	18.482	9.479	19.558
	ω	0.102;-0.102	0.048;-0.048	0.0203;-	0.015;-
	v	0.766	0.721	0.0203 0.79	0.0151 0.774
4	φ	1.797;-3.172	1.527;-0.836	1.374;-1.717	0.422;-1.113
	x	9.891	18.486	9.480	19.562
	ω	0.102;-0.102	0.049;-0.0485	0.0203;-	0.015;-0.015
	v	0.766	0.722	0.0203 0.79	0.774
5	φ	2.970;-2.557	1.896;-2.878	2.315;-3.120	2.119;-1.810
	x	15.233	30.358	15.216	30.327
	ω	0.055;-0.068	0.067;-0.072	0.028;-0.030	0.024;-0.023
	v	1.237	1.248	1.226	1.251
6	φ	2.294;-2.369	2.281;-2.448	0.614;-1.220	1.125;-1.148
	x	15.231	15.259	30.336	30.352
	ω	0.051;-0.052	0.021;-0.028	0.016;-0.029	0.013;-0.018
	v	1.179	1.186	1.219	1.214

Table 2: Results of calculations of full-time and forced acceleration-braking modes of a bridge crane

Model №		Container crane	
		L=10, m; t_p=5, s	L=40, m; t_p=5, s
1	φ	9.326;-11.129	24.868;-17.928
	x	41.387	42.57
	ω	0.284;-0.287	0.442;-0.427
	v	4.359	3.623
2	φ	9.348;-11.269	24.465;-16.303
	x	41.553	36.037
	ω	0.284;-0.283	0.440;-0.427
	v	4.369	3.598
3	φ	4.674;-5.627	4.674;-7.924
	x_1	13.019	19.580
	ω	0.081;-0.081	0.045;-0.038
	v_1	2.185	1.799
4	φ	4.674;-5.633	8.907;-6.346
	x	13.910	14.044
	ω	0.081;-0.081	0.182;-0.169
	v_1	2.175	1.799
5	φ	15.92;-16.57	25.02;-17.66
	x	40.66	41.69
	ω	0.217;-0.213	0.205;-0.124
	v	3.99	4.02
6	φ	8.549;-12.28	8.329;-10.97
	x_1	40.263	36.477
	ω	0.119;-0.147	0.048;-0.108
	v_1	3.797	3.74

44. Conclusion

Different approaches to modeling the dynamics of LHM are considered in the article, namely:

1) using the Lagrange equations of the second kind;

2) using the Lagrange equations of the second kind, with the assumption of small load oscillations;

3) based on using the traditional equations of the trolley-load system with the transition to S.N. Kozhevnikov variables in the integration;

4) based on the traditional trolley-load model, where the deviation of the rope from the vertical is referred to as the movement of the load;

5) modification of the Lagrange equations by replacing the equation of motion of a trolley by the equation similar to the N.S. Haminin equation;

6) using the traditional model, where the equation of motion of a trolley is replaced by the equation similar to the N.S. Haminin equation.

Based on the results of numerical modeling, we can draw conclusions on the level of errors of determining the dynamic characteristics of the trolley-load system on the basis of traditional models vs. the models using the Lagrange equations of the 2nd kind in the regular and forced operation modes:

1. The length of the load suspension has a significant effect on the characteristics of the transients in the crane-load system, which should be taken into account when designing the control to suppress the load oscillations.

2. All the considered calculation models in the regular operation mode of the bridge crane give results varying not more than 1.5 times (Table 1).

3. With accelerated mode of operation of the bridge crane, the calculated dynamic characteristics of the movement of the "trolley-load" system for different models may differ by a factor of 2 (Table 1).

4. Dynamic characteristics in calculating the forced operation mode of the container crane may differ 4 times depending on the mathematical models used (Table 2).

5. To eliminate the adverse operating modes of the "trolley-load" system, the frequency of control action should differ significantly from the frequency of free oscillations of the system.

References

[1] Loveikin VS, Romasevych YO (2017), Dynamic optimization of a mine winder acceleration mode, Issue 4, *Naukovyi Visnyk Natsionalnoho Hirnychoho Universytetu*, pp. 55-61.

[2] Loveikin VS, Chovniuk YuV, Liashko AP (2014), The crane's vibrating systems controlled by mechatronic devices with magnetorheological fluid: The nonlinear mathematical model of behavior and optimization of work regimes, Issue 6, *Naukovyi Visnyk Natsionalnoho Hirnychoho Universytetu*, pp. 97-102.

[3] Hryhorov O, Svirgun V (1986), Improving the productivity of utility cranes through optimum motion control, Vol. 6, *Soviet machine science*, pp. 25-29.

[4] Loveykin VS, Pochka KI (2017), Synthesis of camshaft driving mechanism in roller molding installation with combined motion mode according to acceleration of third order, Vol. 16, Iss. 3, *Science & Technique*, pp. 206-214.

[5] Okun A, Los Y (2016), The controllability function method, Vol. 78, Iss. 3, *U.P.B. Scientific Bulletin. Series D: Mechanical Engineering*, pp. 3–8.